

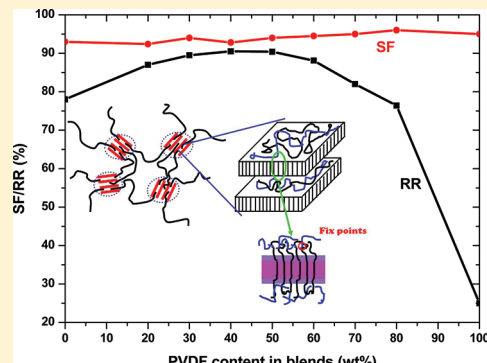
Crystal Orientation Behavior and Shape-Memory Performance of Poly(vinylidene fluoride)/Acrylic Copolymer Blends

Jichun You, Wenyong Dong, Liping Zhao, Xiaojun Cao, Jishan Qiu, Wenjia Sheng, and Yongjin Li*

College of Material, Chemistry and Chemical Engineering, Hangzhou Normal University, No. 16 Xuelin Rd. Hangzhou 310036, China

 Supporting Information

ABSTRACT: The crystal orientation behavior and shape-memory performance of miscible poly(vinylidene fluoride) (PVDF)/acrylic copolymer blends in various ratios have been investigated. With the incorporation of amorphous acrylic copolymer into the gallery of PVDF lamellae, the molecular connection (tie molecule concentration) between the neighboring PVDF crystals decreases gradually. For the blends with more than 80 wt % PVDF, most of the PVDF α -crystals are transformed into β -crystals upon deformation, and the molecular chains of the β -crystals are aligned along the stretching direction because tie molecules transfer the loading effectively. For the blends with less than 30 wt % PVDF, almost all of the PVDF crystals are isolated from each other with very few tie molecules. Mechanical deformation induces the perpendicular crystal molecular chain arrangement with no crystal form transitions. For the blends with 40 wt % to 70 wt % PVDF, the *c*-axis-oriented β -phase and the tilt-oriented α -phase coexist in the uniaxially stretched blends. The shape-memory properties of the blends were also evaluated over the same blend composition range. The maximum shape-memory recovery properties were observed for the blend sample containing 50 wt % PVDF, in which a small amount of tie molecules connect the PVDF crystallites to form a deformable elastic network. This network contributes to the good shape-memory properties of the blend. For the blends with very few tie molecules or high tie molecule concentrations, the deformation induces the slipping of the amorphous molecules or the large fibrillar crystal structure, respectively; thus, these samples exhibit relatively low shape-memory performance.



1. INTRODUCTION

The tie molecules bridging the neighboring crystallites are critically important in determining the mechanical properties of semicrystalline polymers. The crystallites are connected by the tie molecules to form a physically cross-linked network that is critically important for the loading transfer upon deformation.^{1–4} The noncovalent connection between the neighboring crystals due to van der Waals interactions or hydrogen bonding is too weak to transfer the stress upon deformation, and this non-covalent connection results in the brittleness and low strength of semicrystalline polymers. Numerous investigations have been carried out to assess the concentration of tie molecules and to evaluate the tie molecule concentration effects on the mechanical properties of semicrystalline polymers.^{5–9} It was reported that changing the molecular structure and/or varying the crystallization conditions were effective strategies to adjust the concentration of tie molecules in semicrystalline polymers.^{10–14} Such strategies provide a very limited adjustment window of the tie molecule concentration for a certain polymer.

We have proposed a new strategy to adjust the tie molecule concentration using miscible crystalline/amorphous polymer blends with interlamellar structures.¹⁵ In these blends, the molecular chains of the amorphous component are inserted into the lamellar gallery of the crystalline component. The molecular chain incorporation of the amorphous component into the

interlamellar area increases the distance between the adjacent lamellae. Thus, the tie molecule concentration decreases gradually with the insertion of the amorphous component. Previously, we successfully prepared poly(vinylidene fluoride) (PVDF) crystals with very few tie molecules from a miscible blend with an acrylic rubber (ACM) using this strategy. It was further found that the crystals with very few tie molecules show novel molecular chain alignment and exhibit no crystal form transitions upon mechanical deformation.¹⁵

In this paper, an acrylic copolymer with a glass transition temperature of 56 °C was used to fabricate miscible PVDF/acrylic copolymer blends. These blends were used as a thermally induced shape-memory polymer. Systematic investigations were made on the crystal orientation behaviors of a stretching deformation by varying the tie molecule concentrations for the PVDF/acrylic copolymer blend. Attention was especially given to the structure–property relations for such blends upon varying the tie molecule concentrations. It was shown that the tie molecule concentrations not only affect the alignment of the PVDF crystals but also act as a load transfer bridge, inducing PVDF crystal form transformation. More importantly, it was

Received: September 21, 2011

Revised: November 29, 2011

Published: December 22, 2011

found that the PVDF/acrylic copolymer blends with 40–50 wt % of PVDF exhibit excellent shape-memory properties with a switching temperature of approximately 45 °C. The molecular mechanism analysis indicates that the small PVDF crystals in the blends act as the netpoints and that few tie molecules connect these netpoints to form a nice elastic network for the blend. The results obtained open new avenues for fabricating thermoplastic shape-memory polymers using a simple blending method.

2. EXPERIMENTAL SECTION

2.1. Materials and Sample Preparation. The PVDF and acrylic copolymer were kindly provided by Kureha Chemicals, Japan, and Nagase Co., Ltd., respectively. The molecular weight and polydispersity of the PVDF are $M_w = 209\,000$ and $M_w/M_n = 2.0$, respectively, as determined by gel permeation chromatography. The head-to-head unit concentration in the molecule is about 5%, which can be determined by the NMR investigation.¹⁶ The acrylic copolymer is a ternary copolymer of acrylonitrile, ethyl acrylate, and butyl acrylate. The weight-average molecular weight of the acrylic copolymer is $M_w = 287\,000$. The glass transition temperature of the acrylic copolymer is 56 °C, as measured by dynamic mechanical analysis. All of the polymers were dried in a vacuum oven at 80 °C for at least 12 h before processing. Blends with various amounts of PVDF were prepared using a Brabender-type plastic mixer (Toyoseiki Co. KF70 V) with two rotors at a rotation speed of 100 rpm at 190 °C for 10 min. After blending, all of the samples were hot pressed at 200 °C for 5 min into a film with a thickness of 500 μm, which was followed by quenching in ice water. The quenched films were kept in an oven with a temperature of 50 °C for at least 8 h. The obtained films were used for further characterization. The oriented films were prepared using an automatic stretching machine at 75 °C with a draw ratio of 4.0. The strain rate was 200%/min during stretching.

2.2. Characterization. Dynamic mechanical analysis (DMA) was conducted with a RHEOVIBRON DDV-25FP (Orientec Corp.) in the tensile mode. The dynamic storage and loss moduli were determined at a frequency of 1 Hz and a heating rate of 3 °C/min as a function of temperature from −150 to +150 °C. Differential scanning calorimetry (DSC) was conducted under a nitrogen flow at a heating or cooling rate of 10 K/min with a Perkin-Elmer DSC-7 differential scanning calorimeter that was calibrated using the melting temperatures of indium and zinc.

Polarized Fourier transform infrared spectroscopy (FTIR) spectra were obtained at a resolution of 2 cm^{−1} using a Digilab FTS 6000 spectrophotometer and a wire-grid polarizer. The samples for the FTIR measurements were made using the same procedure as those for the X-ray characterization, and the film thicknesses ranged from 10 to 30 μm.

Small angle X-ray scattering (SAXS) patterns were obtained by microfocused Cu Kα radiation (45 kV, 60 mA) generated by an X-ray diffractometer (Rigaku Ultron 4153A 172B) and an imaging plate detector. To obtain the long period and the correlation length (thickness of the amorphous layer and the crystalline layer), the one-dimensional correlation function is calculated according to the classic two phases model.¹⁷ Wide-angle X-ray diffraction (WAXD) profiles were obtained using Cu Kα radiation (40 kV, 120 mA) generated by an X-ray diffractometer (Rigaku, Ultron 8000) with a scanning speed of 1 deg/min.

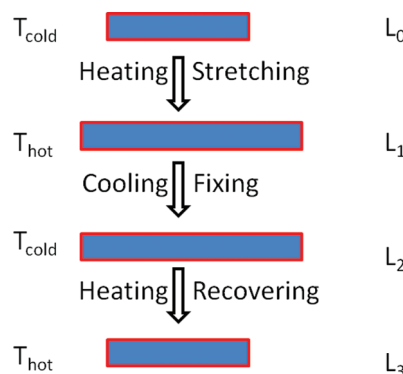


Figure 1. Schematic diagram for the shape memory properties measurements.

WAXD patterns for the stretched samples were obtained using the same X-ray diffractometer with an imaging plate detector.

The structure of the PVDF/acrylic copolymer blend was characterized by transmission electron microscopy (TEM). Thin slices of samples were microtomed using a Reichert Ultracut S (Leica Microsystems Co. Ltd.) at −40 °C. The sections were collected onto a 600-mesh copper grid and were stained with RuO₄ at room temperature for 20 min. The TEM images were observed using a transmission electron microscope (Hitachi 7000) at an accelerating voltage of 75 kV.

2.3. Shape-Memory Properties. Shape-memory property measurements were conducted using samples cut into a rectangular shape. The samples were treated under a specific temperature-deformation program, as schematically depicted in Figure 1. T_{hot} and T_{cold} were the temperatures of the water bath at 75 and 0 °C, respectively. The shape fixity (SF) and recovery ratio (RR) were then determined by

$$SF = \frac{l_2 - l_0}{l_1 - l_0} \times 100\% \quad (1)$$

$$RR = \frac{l_2 - l_3}{l_2 - l_0} \times 100\% \quad (2)$$

3. RESULTS

3.1. Miscibility between PVDF and Acrylic Copolymer. The glass transition temperatures of the PVDF/acrylic copolymer blends were evaluated using dynamic mechanical analysis, as shown in Figure 2. The T_g s of the neat PVDF and neat acrylic copolymer are −40 and +56 °C, respectively. All of the blends show only one glass transition temperature, indicating molecular miscibility between the PVDF and acrylic copolymer over the entire range of compositions. The acrylic copolymer contains many carboxyl groups that have specific interactions with the CF₂ groups of PVDF; these interactions are similar to the interactions of the blends of PVDF with poly(methyl methacrylate) (PMMA)^{18,19} and PVDF with acrylic rubber (ACM).¹⁵ Note that the glass transition temperatures (T_g) of blends with all PVDF contents are close to that of the acrylic copolymer due to the high crystallinity (see the Supporting Information) of PVDF in the blends.

Figure 3 displays the Lorentz-corrected SAXS profiles of the neat PVDF and the PVDF/acrylic copolymer blends in the isotropic state. All SAXS intensities were normalized by thickness

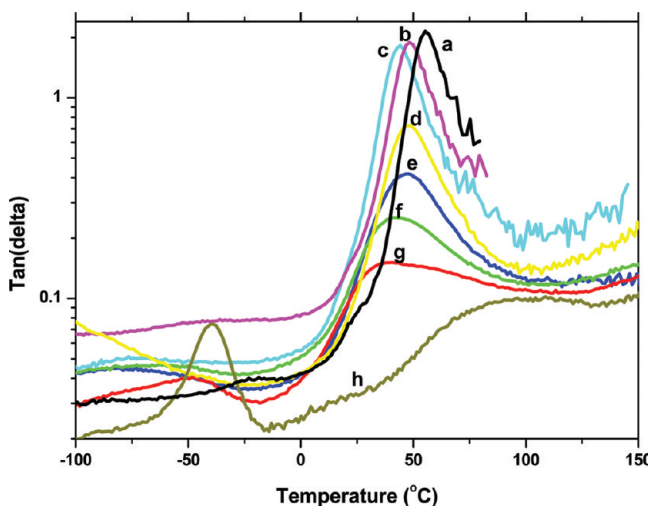


Figure 2. $\tan \delta$ of PVDF/acrylic copolymer blends as a function of temperature: (a) acrylic copolymer; (b) acrylic copolymer/PVDF = 90/10; (c) acrylic copolymer/PVDF = 80/20; (d) acrylic copolymer/PVDF = 60/40; (e) acrylic copolymer/PVDF = 50/50; (f) acrylic copolymer/PVDF = 40/60; (g) acrylic copolymer/PVDF = 20/80; (h) PVDF.

and exposure time after subtracting air scattering from the observed profiles. The neat PVDF exhibits a weak scattering peak at $q = 0.55 \text{ nm}^{-1}$, corresponding to a crystal long period of 11.4 nm. With the addition of amorphous acrylic copolymer into the PVDF, the scattering peak shifts to the low angle direction, indicating an increased PVDF crystal long period, as indicated in Figure 4. However, the scattering peak intensity increases significantly by blending with the acrylic copolymer, which signifies an increased density difference between the amorphous region and the crystalline region in the blends. This density difference is attributed to the much lower density of acrylic copolymer compared to PVDF (the densities of acrylic copolymer and PVDF are 1.25 and 1.78 g/cm^3 , respectively). Both of features indicate the incorporation of amorphous acrylic copolymer chains into the gallery between the PVDF lamellae.

3.2. Crystal Forms of PVDF in the Oriented Blends. PVDF is a typical polymorphic polymer.^{20–23} Numerous investigations have reported the α - to β -crystal form transitions upon stretching deformations. Polarized FTIR spectroscopy was used to determine the crystal forms of PVDF and the molecular chain alignment of each crystal form. Polarized FTIR spectra of PVDF/acrylic copolymer blends with the indicated compositions at the draw ratio of 4.0 are shown in Figure 5. Only the α -phase is observed for the blends with less than 30 wt % PVDF because the characteristic spectrum of α -PVDF was obtained, showing well-defined absorption bands at 532, 614, 764, 796, 855, and 976 cm^{-1} . As the PVDF content increases, the intensities of the characteristic α -phase bands decrease and those of the bands at 510 and 840 cm^{-1} (characteristic of the β -phase) increase. For the neat PVDF, only the characteristic absorptions of the β -phase were observed with the draw ratio of 4.0, indicating the full crystal α - to β -transformation by the stretching.²³ It is well-known that the PVDF TGTG[−] α -phase converts into the polar all-*trans* β -phase upon mechanical deformation below 100 °C.^{24,25} The results shown here indicate that the incorporation of acrylic copolymer impedes the crystal α - to β -transformation in the blends.

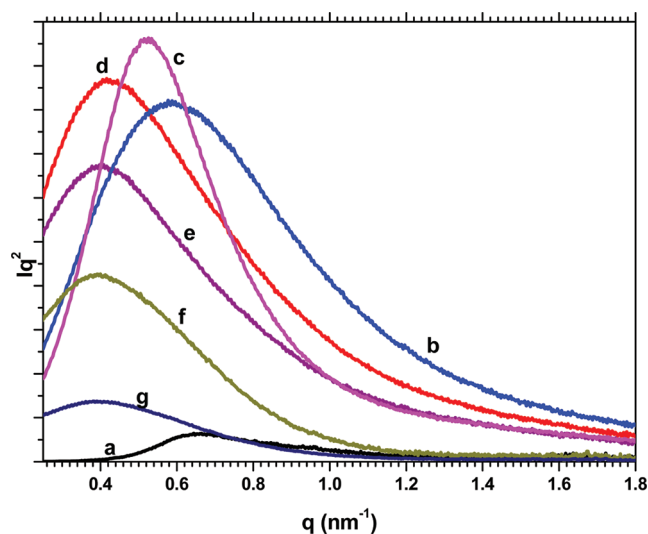


Figure 3. Lorentz-corrected SAXS profiles for (a) neat PVDF, (b) ACM/PVDF = 80/20, (c) ACM/PVDF = 70/30, (d) ACM/PVDF = 60/40, (e) ACM/PVDF = 50/50, (f) ACM/PVDF = 40/60, (g) ACM/PVDF = 20/80.

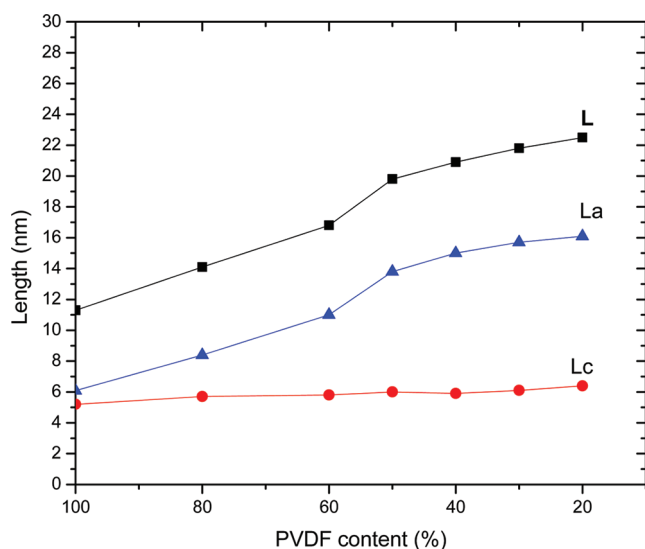


Figure 4. Long period (L), thickness of the crystalline layer (L_c), and thickness of the amorphous layer (L_a) for the PVDF/acrylic copolymer blends.

The molecular chain orientation behavior of each crystal phase can also be detected by the polarized FTIR measurements. The characteristic α -peak at 532 cm^{-1} has been assigned to the CF_2 (52%) mode and the characteristic β -peak at 510 cm^{-1} has been assigned to the CF_2 (98%) mode.²⁶ Therefore, the two peaks were used for the crystal orientation study by polarized FTIR. It is shown in Figure 5 that the parallel peak intensity of the 510 cm^{-1} characteristic peak is always stronger than the perpendicular peak intensity. The results indicate that the molecular chains of the β -phase in the blends are stretched parallel to the stretching direction independent of the compositions in the blends. However, for those absorption bands of the α -phase, a different orientation behavior can be observed with a change in the compositions. It was found that the parallel intensity ($R_{||}$)

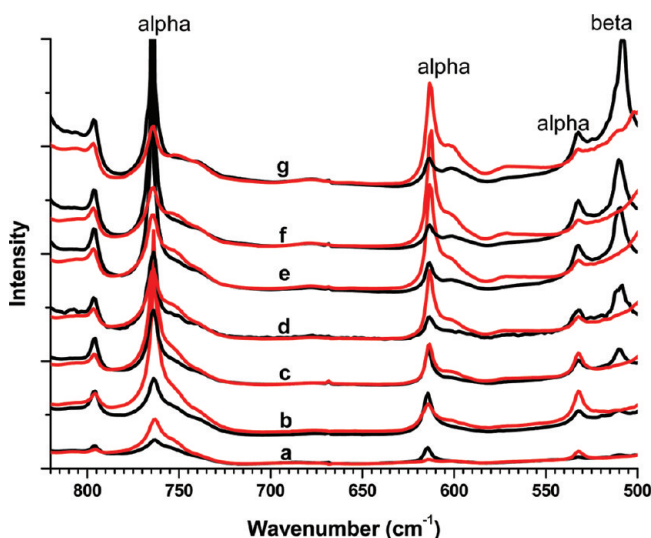


Figure 5. Polarized FTIR spectra of (a) ACM/PVDF = 80/20, (b) ACM/PVDF = 70/30, (c) ACM/PVDF = 60/40, (d) ACM/PVDF = 50/50, (e) ACM/PVDF = 60/40, (f) ACM/PVDF = 70/30, and (g) ACM/PVDF = 20/80 (black lines are the parallel direction spectra, red lines are the perpendicular direction spectra).

at 532 cm^{-1} is higher than the vertical intensity (R_{\perp}) with a low PVDF concentration, but the vertical intensity increases gradually with increasing PVDF content.²⁷ For the 40–50 wt % PVDF samples, no dichroism on the characteristic α -absorption bands can be observed from the polarized FTIR measurements. Upon further increasing the content of PVDF, the parallel intensity becomes weaker than the perpendicular intensity, as shown in Figure 6. It is obvious that the molecular alignment changed from the vertical direction to the parallel direction in the α -crystals with an increase in the PVDF content. In other words, the dichroism behavior of the characteristic absorption bands of the PVDF crystals in the blends indicates that all of the molecular chains of the β -phase are always aligned along the stretch direction and that the molecular chains of the α -crystal are gradually transformed from the vertical direction to the parallel direction with increasing PVDF content in the blends. This result is confirmed by the WAXD results in the following section.

3.3. Crystal Lamellar Alignment upon Orientation. The crystal orientation of the PVDF/acrylic copolymer blends with various component ratios has been characterized using WAXD and SAXS. Figure 7 displays the SAXS and WAXD patterns of the oriented blends with various compositions (all blends have a draw ratio of 4.0). To aid in the visualization of the PVDF crystallite distribution, the hypothesized morphologies are shown adjacent to the SAXS and WAXD patterns in Figure 7.

For the blends with less than 30 wt % PVDF, the SAXS patterns show no scattering peaks in the meridional direction, but they do show strong scattering peaks in the equatorial direction (Figure 7c). This pattern indicates the electron density difference along the stretching direction, which means that all of the crystals are aligned along the stretching direction. The corresponding WAXD patterns show the typical α -form diffractions with the (020) reflection on the meridional direction (Figure 7c'). These results are also consistent with the FTIR measurements. As previously reported,¹⁵ the large amount of amorphous acrylic

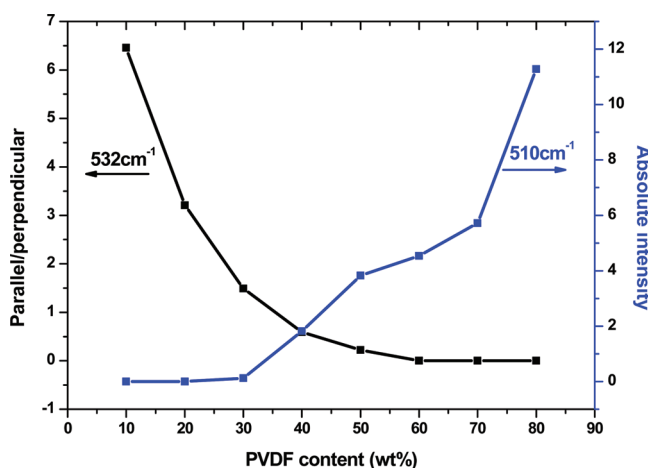


Figure 6. Absorption intensity parallel/perpendicular ratio for the α -crystal characteristic peak and the absolute intensity for the β -crystal characteristic peak as a function of the PVDF content in the blend.

copolymer incorporation leads to the isolation of the PVDF crystallites. The stress cannot be transferred into the inside of the PVDF crystals, so no crystal transformation occurs. These isolated PVDF lamellae were oriented vertical to the stretching direction by the mechanical deformation.

With increasing PVDF content, different SAXS patterns were observed when the PVDF content ranges between 40 and 70 wt %, as shown in Figure 7b. The SAXS patterns exhibit a six-point pattern with two equatorial scatterings and four tilt scatterings. The corresponding WAXD results indicate that all of these samples show the α - and β -crystal mixtures. The β -PVDF crystals are highly oriented with the molecular chain along the stretch direction, but the α -PVDF crystals show relatively low orientation functions, as indicated by the arched α -reflection peaks. Considering the relatively low tie molecule concentration of the PVDF crystallites in this range, a hypothesized crystal arrangement has been proposed, as shown in Figure 7b'). The crystals in the blends connected by the tie molecules before stretching are subjected to mechanical deformations; thus, α -crystals are transformed into the β -phase. Simultaneously, the crystals were also aligned with the molecular chains along the stretching direction for the transformed β -phase. For the other crystals with very few tie molecules, the stretching shear force renders the tilt alignment of these crystals, leading to the four-point scattering in the SAXS patterns. These crystals are the α -crystals with no crystal transformations because no direct stress has been applied inside the crystallites.

For the blends with more than 80 wt % PVDF, only meridional scattering peaks in the SAXS pattern can be observed (Figure 7a), indicating that the crystal lamellae are aligned vertical to the stretching direction. This alignment is seen for most semicrystalline polymers. The molecular chains are oriented along the stretching direction with uniaxial orientation. The corresponding WAXD patterns show that the PVDF is mainly in the β -crystal form and that all $h00$ diffractions of the PVDF crystals are only located in the equatorial direction. The results again mean that the PVDF molecular chains are parallel to the stretch direction. This orientation behavior is attributed to the polymer lamellae, which are tightly connected by tie molecules. The tie molecules can transfer the stress from the

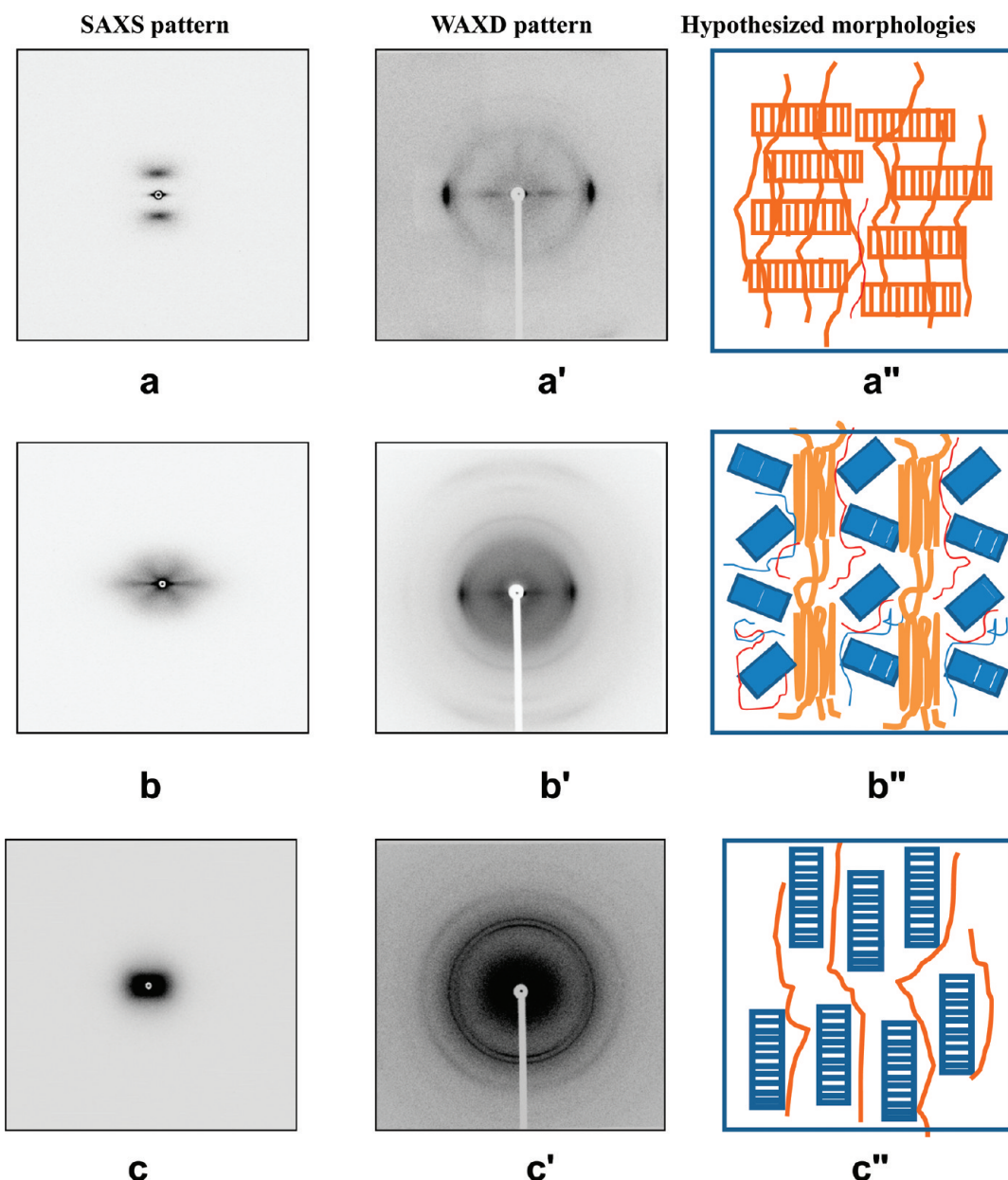


Figure 7. SAXS, WAXD and hypothesized morphologies of PVDF/acrylic copolymer blends: (a) for the blends with PVDF more than 80 wt%; (b) for the blends with PVDF range from 30 to 80 wt%; (c) for the blends with less than 30 wt % PVDF.

amorphous part to the crystalline part very effectively. Therefore, deformation by stretching induces the fibrillar transformation of PVDF crystals. The fibrillar transformation draws the chains along the stretch axis, and the crystal blocks are then normal to the stretch direction.

3.4. Shape-Memory Properties. Shape-memory polymers have received increasing attention due to their low density, high deformation strain, good processability, and tunable transition temperatures.^{28–31} In principle, thermally induced shape-memory polymers should have at least two phases on the molecular level: a fixed phase and a thermally reversible phase.³² Most current shape-memory polymers are covalently linked polymers or microphase-separated block copolymers. Miscible crystalline/amorphous polymer blends with sharp glass transition temperatures (higher than room temperature) and low crystallinity are

good candidates for shape-memory polymers. It is thought that the small crystals act as the netpoints to fix the shape, and the molecules between the crystals act as the switching segments for the shape recovery.

We have found that some of the PVDF/acrylic copolymer blends investigated exhibit nice shape-memory properties. Figure 8 shows the shape fixity (SF) and shape recovery ratio (RR) as a function of the blend component ratio. It is seen that all samples show shape fixity higher than 95%. Between samples, the shape fixity is almost constant and is not dependent on the blend compositions. However, the recovery ratios of the PVDF/acrylic copolymer blends show strong blend composition dependence. The highest recovery property was observed at approximately 50 wt % PVDF, and the corresponding RR for that sample is approximately 87%. Considering the large prestrain of 150% for

the sample, the shape-memory performance of the blend is good. Figure 2e shows the DMA curves of the PVDF/acrylic copolymer 50/50 blend. It was found that the sample displays a very sharp glass transition at approximately 45 °C, which is the switching temperature of the shape-memory polymer.

The Supporting Information presents the shape-memory process of the blends with a temporary helical-shaped sample in a water bath at 75 °C. It shows that the shape recovery finishes within 3 s with a very high recovery ratio.

4. DISCUSSION

We observed at least three different PVDF crystal orientation textures in the PVDF/acrylic copolymer blends upon changing the blend compositions with a constant draw ratio of 4.0. This result can be attributed to the tie molecule concentration effects during mechanical stretching. The tie molecule fraction (P) has been estimated using the Huang and Brown

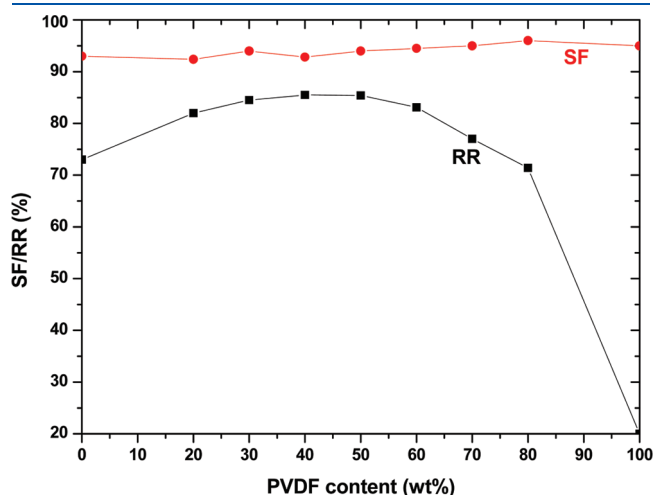


Figure 8. Shape fixity and recovery ratio of PVDF/acrylic copolymer blends as functions of PVDF content.

method:⁸

$$P = \frac{1}{3} \frac{\int_L^\infty r^2 \exp(-b^2 r^2) dr}{\int_0^\infty r^2 \exp(-b^2 r^2) dr} \times \chi \quad (3)$$

Here L is the critical distance required to form a tie molecule, r is the probability of a given end-to-end distance, $b^2 = 3/2\bar{r}^2$ (\bar{r} is the root-mean-square value of the end-to-end distance of a random coil), and χ is the volume fraction of the crystalline component in the miscible blends. To build up intercrystalline tie molecules, the chain segments have to be long enough to span an amorphous layer and the two adjacent crystalline lamellae; chain segments must be longer than the critical distance $L = 2L_c + L_a$, where L_c is the crystal lamellar thickness and L_a is the amorphous layer thickness. The calculated results for the blends and the corresponding orientation behaviors are shown in Figure 9. A high concentration of tie molecules between the crystals transfers the mechanical stress effectively and induces the chain conformation transformation in the crystals (i.e., the α - to β -crystal transition). Simultaneously, the crystal molecular chain was aligned along the stretching direction. In contrast, due to the very low concentration of tie chain molecules in the acrylic copolymer-dominant blends, no tensile loading can be exerted on the PVDF crystals. Therefore, the PVDF maintains the α -phase, and the crystallites entirely rotate to align the molecular chains vertical to the stretch direction. When the tie molecule concentration is intermediate to these two extremes, an intermediate state (as depicted in Figure 7c'') was obtained. In this state, the β -phase is highly oriented along the stretching direction, and the α -phase is tilted with the stretching direction, as shown by SAXS, WAXD, and polarized FTIR.

It is also very interesting to note that the simple melt-mixed PVDF/acrylic copolymer blends with of approximately 40 to 50 wt % PVDF exhibit good shape-memory performance. The shape-memory properties are explained schematically in Figure 10.

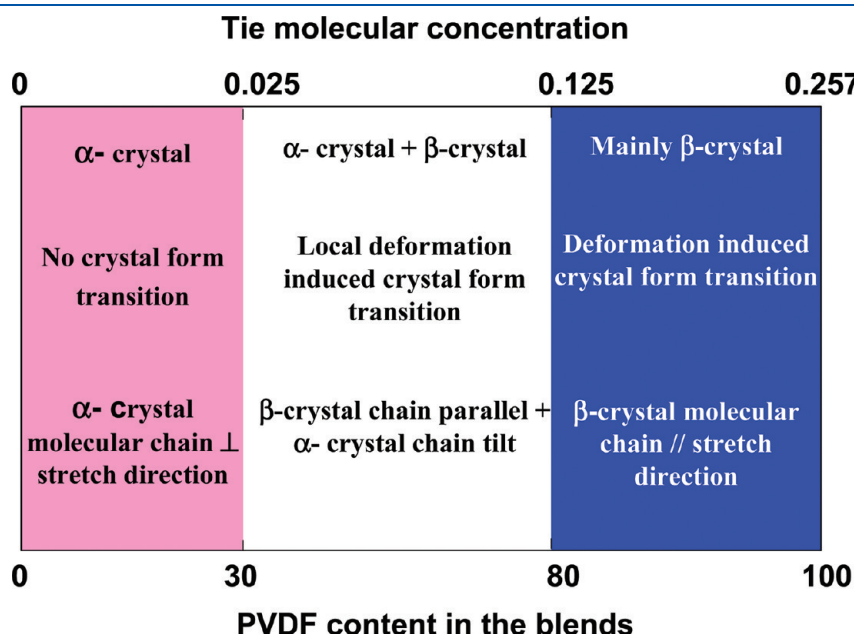


Figure 9. Relationships between the tie molecular concentrations and the orientation behaviors of the blends.

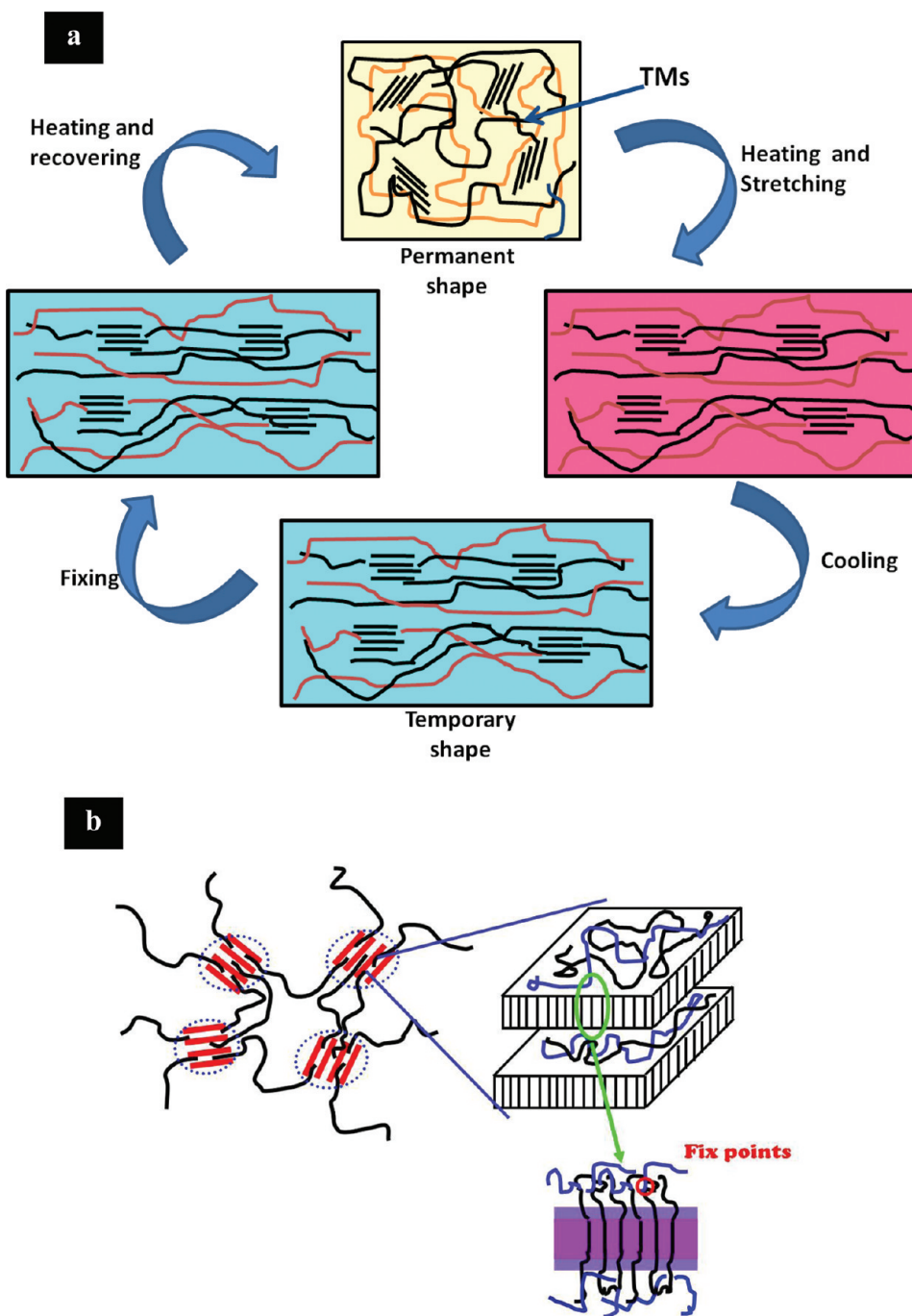


Figure 10. Schematic diagrams for (a) the shape memory properties of PVDF/acrylic copolymer blends; (b) molecular mechanism.

The small PVDF crystals in the blends act as the fixed phase, and the amorphous chains between the PVDF crystals act as the switching parts. When the temperature is higher than the T_g of the blend, the material is soft and ready for deformation. The deformation is fixed by the small PVDF crystals. When the deformed sample is cooled down again, the molecular chains between the PVDF crystals were frozen. When the specimen was heated to a temperature higher than the T_g , the elongated chain recovered due to the entropy elasticity (Figure 10a). The function of the tie molecules between the fixing PVDF crystal phases should be noted. We consider that the small amount of tie molecules between the PVDF crystals is critically important to

the shape recovery properties. The PVDF crystals connected by tie molecules form a very loose and elastic network. The tie molecules prevent molecular slip upon deformation, and the small PVDF crystals act as the fixed phase for the shape-memory performance (Figure 10b). Figure 11 shows the TEM image for the PVDF/acrylic copolymer blend with 50% PVDF. Very thin and short lamellar fragments are observed, and these tiny crystals act as the net points for the shape-memory properties. The SAXS patterns during one shape-memory process are shown in Figure 12. Although the crystal alignment still can be observed after one shape-memory cycle, it is evident that most of the crystal orientation recovered. The results indicate the nice elasticity of

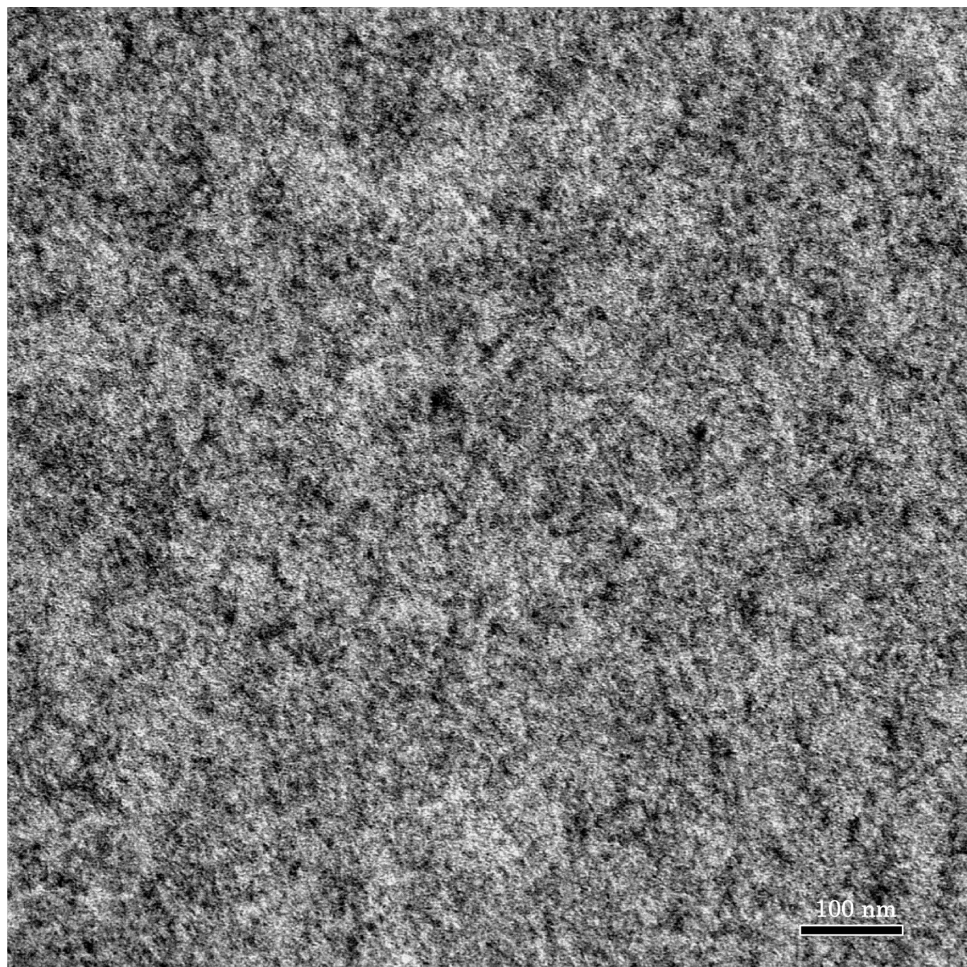


Figure 11. TEM micrographs of PVDF crystallites in PVDF/acrylic copolymer = 50/50.

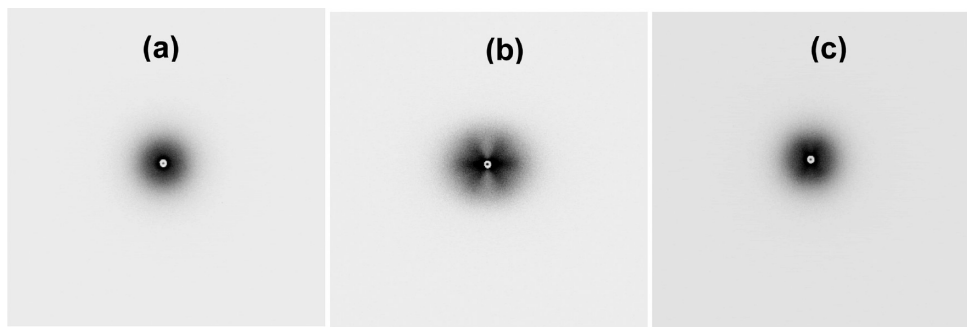


Figure 12. SAXS patterns at the different stages in one shape memory cycle for PVDF/acrylic copolymer = 50/50 blend: (a) before programming; (b) fixing at room temperature after stretching at 75 °C with draw ration of 1.5; (c) after the recovery from the deformed state.

the sample, which is physically cross-linked by the tiny PVDF crystals due to the tie molecules. For the blends with less than 30 wt % PVDF, the PVDF crystals are isolated from each other and are embedded in the amorphous matrix. The mechanical stretching induces the molecular slipping of the amorphous matrix and results in significant permanent deformation. For the blends with PVDF as the major component, PVDF usually crystallizes into large spherulites; this crystallization breaks the structure and leads to permanent deformation upon mechanical deformation.

Furthermore, for samples with many tie molecules connecting the neighboring PVDF crystallites, deformation usually results in a fibrillar structure that cannot be recovered at high temperature.

5. CONCLUSIONS

In summary, we have demonstrated the tie molecule concentration effects on the structure and properties of miscible PVDF/acrylic copolymer blends. It was found that crystal

transformation by mechanical deformation can only occur when the stress can be transferred inside of polymer crystals by tie molecules. Furthermore, it was found that tiny PVDF crystals connected by a small amount of tie molecules act as the fixing phase, leading to an excellent shape-memory polymer. The strategy presented here opens a new avenue for fabricating new thermoplastic shape-memory polymers.

■ ASSOCIATED CONTENT

S Supporting Information. Video showing the shape recovery properties of PVDF/acrylic copolymer (=50/50) blend, where the permanent shape is straight strand and the temporary shape is the helical curve, and a table showing the thermal behaviors of the blends. This material is available free of charge via the Internet at <http://pubs.acs.org>

■ AUTHOR INFORMATION

Corresponding Author

*E-mail: yongjin_li@yahoo.com. Telephone: 86-571-2886-6579. Fax: 86-571-2886-7899.

■ ACKNOWLEDGMENT

This study was partially supported by the National Science Foundation of China (21074029), Zhejiang Provincial Natural Science Foundation of China (R4110021) and the Project of Zhejiang Key Scientific and Technological Innovation Team (2010R50017).

■ REFERENCES

- (1) Keith, H. D.; Paden, F. J., Jr.; Vadimsky, R. G. *J. Polym. Sci. Part A-2: Polym. Phys.* **1966**, *4*, 267–281.
- (2) Friedrich, K. *Adv. Polym. Sci.* **1983**, *52*, 225–227.
- (3) Shah, A.; Stepanov, E. V.; Capaccio, G.; Hiltner, A.; Baer, E. *J. Polym. Sci., Part B: Polym. Phys.* **1998**, *36*, 2355–2369.
- (4) Seguela, R. *J. Polym. Sci., Part B: Polym. Phys.* **2005**, *43*, 1729–1748.
- (5) Peterlin, A. *J. Macromol. Sci. Phys.* **1973**, *7*, 705–727.
- (6) Brown, N.; Ward, I. M. *J. Mater. Sci.* **1983**, *18*, 1405–1420.
- (7) Haward, R. N. *J. Polym. Sci., Part B: Polym. Phys.* **1995**, *33*, 1481–1494.
- (8) (a) Huang, Y. L.; Brown, N. *J. Mater. Sci.* **1988**, *23*, 3648–3655. (b) Huang, Y. L.; Brown, N. *J. Polym. Sci., Part B: Polym. Phys.* **1990**, *28*, 2007–2021. (c) Huang, Y. L.; Brown, N. *J. Polym. Sci., Part B: Polym. Phys.* **1991**, *29*, 129–137.
- (9) Lustiger, A.; Ishikawa, N. *J. Polym. Sci., Part B: Polym. Phys.* **1991**, *29*, 1047–1055.
- (10) Uehara, H.; Matsuda, H.; Aoike, T.; Yamanobe, T.; Komoto, T. *Polymer* **2001**, *42*, 5893–5903.
- (11) Zhang, M. Z.; Yuen, F.; Choi, P. *Macromolecules* **2006**, *39*, 8517–8522.
- (12) Shen, F. W.; McKellop, H. A.; Salovey, R. *J. Polym. Sci., Part B: Polym. Phys.* **1996**, *34*, 1063–1077.
- (13) Nitta, K. H.; Takayanagi, M. *J. Polym. Sci., Part B: Polym. Phys.* **1999**, *37*, 357–368.
- (14) Takayanagi, M.; Nitta, K. *Macromol. Theory Simulations* **1997**, *6*, 181–195.
- (15) Li, Y. J.; Iwakura, Y.; Shimizu, H. *Macromolecules* **2008**, *41*, 3396–3400.
- (16) Holstein, P.; Scheler, U.; Harris, R. K. *Polymer* **1998**, *39*, 4937–4941.
- (17) Strobl, G. R.; Schneider, M. *J. Polym. Sci., Part B: Polym. Phys.* **1980**, *18*, 1343–1359.
- (18) Nishi, T.; Wang, T. T. *Macromolecules* **1975**, *8*, 909–915.
- (19) Bernstein, R. E.; Paul, D. R.; Barlow, J. W. *Polym. Eng. Sci.* **1978**, *18*, 683–686.
- (20) Gregorio, R.; Capitao, R. C. *J. Mater. Sci.* **2000**, *35*, 299–306.
- (21) Lovinger, A. J. *J. Polym. Sci. Polym. Phys. Ed* **1980**, *18*, 793–809.
- (22) Morra, B. S.; Stein, R. S. *J. Polym. Sci., Part B: Polym. Phys.* **1982**, *20*, 2243–2259.
- (23) Lovinger, A. J. *Polymer* **1980**, *21*, 1317–1322.
- (24) Hsu, T. G.; Geil, P. H. *J. Mater. Sci.* **1989**, *24*, 1219–1232.
- (25) Takahashi, Y.; Matsubara, Y.; Tadokoro, H. *Macromolecules* **1983**, *16*, 1588–1592.
- (26) Kobayashi, M.; Tashiro, K.; Tadokoro, H. *Macromolecules* **1975**, *8*, 158–162.
- (27) Palm, K. *Vibr. Spectrosc.* **1994**, *6*, 185–193.
- (28) Xie, T. *Nature* **2010**, *464*, 267–270.
- (29) Wang, W.; Jin, Y.; Ping, P.; Chen, X.; Jing, X.; Su, Z. *Macromolecules* **2010**, *43*, 2942–2948.
- (30) Kolesov, I. S.; Kratz, K.; Lendlein, A.; Radusch, H. J. *Polymer* **2009**, *50*, 5490–5498.
- (31) Liu, C.; Chun, S. B.; Materh, P. T.; Zheng, L.; Haley, E. H.; Coughlin, E. B. *Macromolecules* **2002**, *35*, 9868–9874.
- (32) Lendlein, A.; Kelch, S. *Angew. Chem., Int. Ed.* **2002**, *41*, 2034–2057.